Chapter 9: Boundary Layer (Pope 7.3)

Part 1

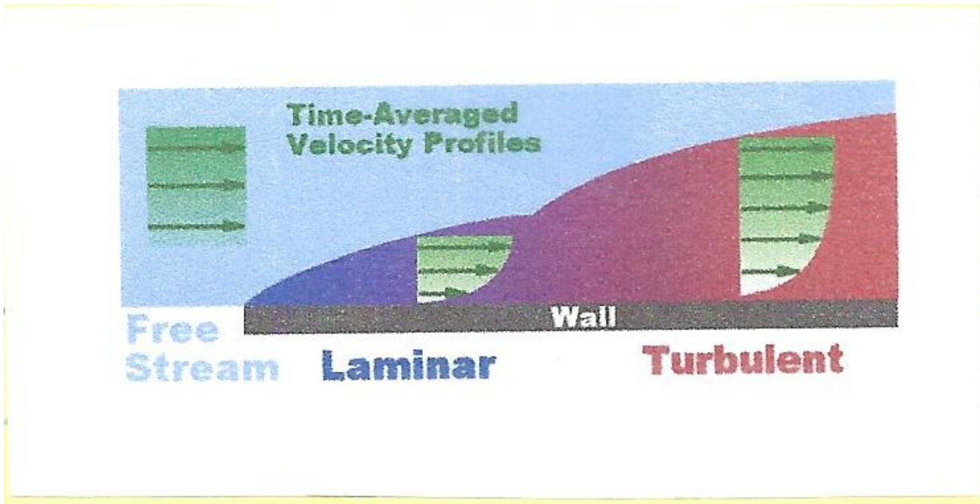

Differences channel/pipe flows:

1) $\delta(x)$
2) $\tau_w(x)$ not known a priori
3) Intermittency

Nonetheless, inner layer $y/\delta(x) < 0.1$ is the same as channel/pipe flows. Some differences in the log law and especially defect layer as departure from log law is more significant.

For boundary layer flow:

$$\underline{U} = (U, V, W) \quad \langle W \rangle = 0$$

Outside BL $p_0(x)$ and $U_0(x)$ are linked by Bernoulli's equation for inviscid flow:

$$-p_0(x) + \frac{1}{2}\rho U_0(x)^2 = \text{constant}$$

Such that the pressure gradient is given by:

$$-\frac{dp_0}{dx} = \rho U_0 \frac{dU_0}{dx}$$

$U_{0_x} > 0$ accelerating flow, i.e., favorable $p_{0_x} < 0$

$U_{0_x} < 0$ decelerating flow, i.e., adverse $p_{0_x} > 0 \rightarrow$ leads to BL separation.

Boundary layer thickness $\delta(x)$ defined as the value of y at which:

$$\langle U(x, y)\rangle = 0.99 U_0(x)$$

Displacement thickness:

$$\delta^*(x) \equiv \int_0^\infty \left(1 - \frac{\langle U\rangle}{U_0}\right) dy$$

$$Q\int_{\delta^*}^{\delta} (\text{inviscid flow}) = Q\int_0^{\delta} (\text{viscous flow})$$

i.e.,

$$\int_{\delta^*}^{\delta} U_0 dy = \int_0^{\delta} \langle U\rangle dy$$

Displacement thickness used in viscous/inviscid intersection approaches: measure of amount inviscid flow displaced due to BL.

Momentum thickness:

$$\theta(x) \equiv \int_0^\infty \frac{\langle U\rangle}{U_0}\left(1 - \frac{\langle U\rangle}{U_0}\right) dy$$

Measure of loss of momentum due to BL.

Various Reynolds numbers:

$$Re_x = \frac{U_0 x}{\nu} \quad Re_\delta = \frac{U_0 \delta}{\nu} \quad Re_{\delta^*} = \frac{U_0 \delta^*}{\nu} \quad Re_\theta = \frac{U_0 \theta}{\nu}$$

$Re_x \sim 10^6$ represents Re_{crit} for transition.

Continuity Equation:

$$\frac{\partial U}{\partial x} + \frac{\partial V}{\partial y} = 0$$

Mean momentum equations:

Mean axial momentum equation for BL flow:

$$\langle U\rangle \frac{\partial \langle U\rangle}{\partial x} + \langle V\rangle \frac{\partial \langle U\rangle}{\partial y} = -\frac{1}{\rho}\frac{d\langle p\rangle}{dx} + \nu\left[\cancel{\frac{\partial^2 \langle U\rangle}{\partial x^2}} + \frac{\partial^2 \langle U\rangle}{\partial y^2}\right] - \cancel{\frac{\partial \langle u^2\rangle}{\partial x}} - \frac{\partial \langle uv\rangle}{\partial y}$$

Mean lateral momentum equation:

$$\cancel{\langle U\rangle \frac{\partial \langle V\rangle}{\partial x}} + \cancel{\langle V\rangle \frac{\partial \langle V\rangle}{\partial y}} = -\frac{1}{\rho}\frac{d\langle p\rangle}{dy} + \nu\left[\cancel{\frac{\partial^2 \langle V\rangle}{\partial x^2}} + \cancel{\frac{\partial^2 \langle V\rangle}{\partial y^2}}\right] - \frac{\partial \langle v^2\rangle}{\partial y} - \cancel{\frac{\partial \langle uv\rangle}{\partial x}}$$

$$\frac{1}{\rho}\frac{d\langle p\rangle}{dy} + \frac{\partial \langle v^2\rangle}{\partial y} = 0$$

Integrating between 0 and ∞, and using the conditions $p = p_0(x)$, $\langle v^2\rangle = 0$ for $y \to 0\ and\ \infty$, since at the wall p(x) = p_w(x)= p_0(x) as it does at ∞

$$\frac{\langle p\rangle}{\rho} = \frac{p_0}{\rho} - \langle v^2\rangle \quad (1)$$

Differentiating Eq. (1) with respect to x yields:

$$\frac{1}{\rho}\frac{\partial \langle p\rangle}{\partial x} = \frac{1}{\rho}\frac{\partial p_0}{\partial x} - \frac{\partial \langle v^2\rangle}{\partial x}$$

${p_0}_x = 0$ flat plate or ${p_0}_x = \rho U_0 {U_0}_x$ for BL with pressure gradient.

Mean axial momentum equation not specialized to BL:

$$\langle U\rangle\frac{\partial\langle U\rangle}{\partial x}+\langle V\rangle\frac{\partial\langle U\rangle}{\partial y}=-\frac{1}{\rho}\frac{dp_0}{dx}+\underbrace{\nu\frac{\partial^2\langle U\rangle}{\partial y^2}}_{\boxed{1}}-\frac{\partial\langle uv\rangle}{\partial y}-\underbrace{\frac{\partial}{\partial x}(\langle u^2\rangle-\langle v^2\rangle)}_{\boxed{2}}$$

Term 1: is proportional to Re^{-1}, and is therefore negligible, except very near wall.
Term 2: usually neglected but can be appreciable for free shear flows.

For BL:

$$\langle U\rangle\frac{\partial\langle U\rangle}{\partial x}+\langle V\rangle\frac{\partial\langle U\rangle}{\partial y}=-\frac{1}{\rho}\frac{d\langle p\rangle}{dx}+\nu\frac{\partial^2\langle U\rangle}{\partial y^2}-\frac{\partial\langle uv\rangle}{\partial y}\qquad(2)$$
$$=\frac{1}{\rho}\frac{\partial\tau}{\partial y}+U_0\frac{dU_0}{dx}$$

Where $\tau(x,y)$ is the total shear stress

$$\tau=\rho\nu\frac{\partial\langle U\rangle}{\partial y}-\rho\langle uv\rangle$$

At the wall, LHS of Eq. (2) is zero, i.e., pressure gradient and shear stress balance. If pressure gradient is zero, then:

$$\frac{1}{\rho}\frac{\partial\tau}{\partial y}=\left.\nu\frac{\partial^2\langle U\rangle}{\partial y^2}\right|_{y=0}=0$$

Since $\langle uv\rangle\sim y^3$.

Eq. (2) can be integrated to obtain von Karman's integral momentum equation. For zero pressure gradient:

$$\tau_w=\frac{d}{dx}(\rho U_0^2\theta)=\rho U_0^2\frac{d\theta}{dx}$$

Or, for the skin friction coefficient,

$$c_f \equiv \frac{\tau_w}{\frac{1}{2}\rho U_0^2} = 2\frac{d\theta}{dx}$$

For laminar zero pressure gradient boundary layer, Blasius similarity solution:

$$\frac{\delta}{x} \approx 4.9Re_x^{-1/2}, \quad \frac{\delta^*}{\delta} \approx 0.35, \quad \frac{\theta}{\delta} \approx 0.14 \quad c_f \equiv 0.664Re_x^{-1/2}$$

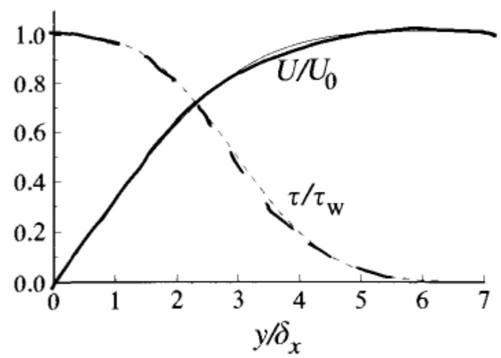

Fig. 7.25. Normalized velocity and shear-stress profiles from the Blasius solution for the zero-pressure-gradient laminar boundary layer on a flat plate: y is normalized by $\delta_x \equiv x/\mathrm{Re}_x^{1/2} = (x\nu/U_0)^{1/2}$.

Mean velocity profiles.

$Re_\theta = 8000$

$H = \dfrac{\delta^*}{\theta} = \text{shape factor}$

Blasius $H \approx 2.6$

Turbulent flat plate BL $H \approx 1.3$

H measures flatness $\langle U \rangle$ away from wall: increased flatness $H \downarrow$

$\langle U \rangle$ similar channel flow

τ/τ_w like laminar profile.

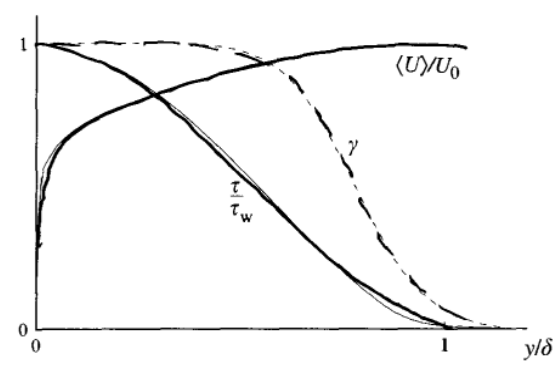

Fig. 7.26. Profiles of the mean velocity, shear stress and intermittency factor in a zero-pressure-gradient turbulent boundary layer, $\mathrm{Re}_\theta = 8{,}000$. (From the experimental data of Klebanoff (1954).)

Law of the wall

$$u^+ = \frac{\langle U \rangle}{U_\tau} \quad y^+ = \frac{y}{\delta_\nu} = \frac{yU_\tau}{\nu}$$

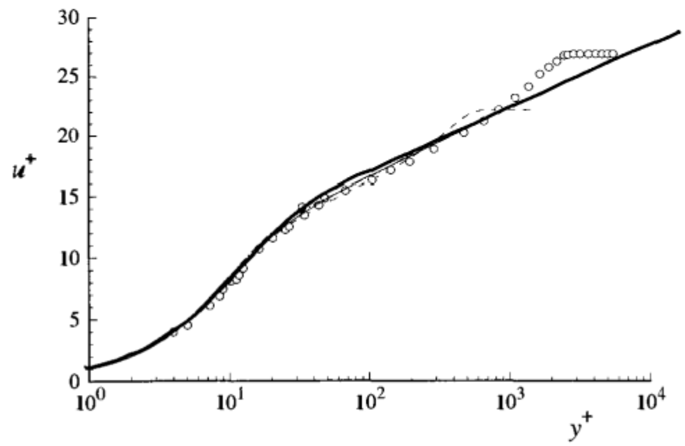

Fig. 7.27. Mean velocity profiles in wall units. Circles, boundary-layer experiments of Klebanoff (1954), $Re_\theta = 8{,}000$; dashed line, boundary-layer DNS of Spalart (1988), $Re_\theta = 1{,}410$; dot–dashed line, channel flow DNS of Kim *et al.* (1987), Re = 13,750; solid line, van Driest's law of the wall, Eqs. (7.144)–(7.145).

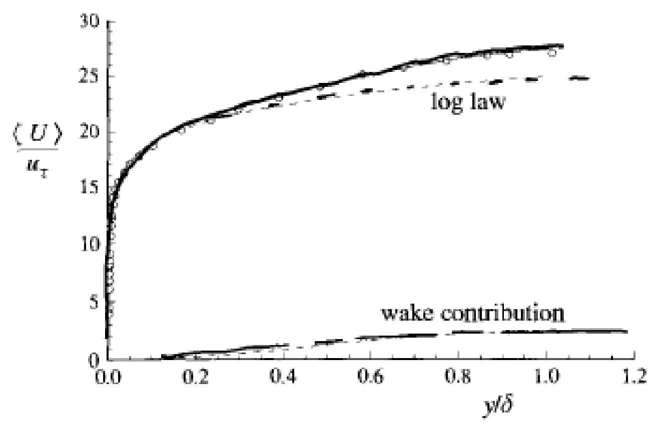

Fig. 7.28. The mean velocity profile in a turbulent boundary layer showing the law of the wake. Symbols, experimental data of Klebanoff (1954); dashed line, log law ($\kappa = 0.41, B = 5.2$); dot–dashed line, wake contribution $\Pi w(y/\delta)/\kappa$ ($\Pi = 0.5$); solid line, sum of log law and wake contribution (Eq. (7.148)).

1) $y^+ < 5 \rightarrow u^+ = f_w(y^+) \approx y^+$
2) $5 < y^+ < 30$ buffer layer
3) $y^+ > 30$ and $y/\delta < 0.3$ log law, while $y/\delta > 0.3$ velocity deficit law

EFD and DNS follow 1,2,3.

What is the form of $u^+ = f_w(y^+)$ in buffer layer?

Note $f_w(y^+) = y^+ - \frac{(y^+)^2}{2R_\tau} - \frac{\sigma(y^+)^4}{4}$ (Pope Ex. 7.9)

Using mixing-length hypothesis, total shear stress is

$$\frac{\tau(y)}{\rho} = \nu\frac{\partial\langle U\rangle}{\partial y} - \langle uv\rangle$$

$$= \nu\frac{\partial\langle U\rangle}{\partial y} + \nu_t\frac{\partial\langle U\rangle}{\partial y}$$

$$= \nu\frac{\partial\langle U\rangle}{\partial y} + l_m^2\left(\frac{\partial\langle U\rangle}{\partial y}\right)^2 \quad (3)$$

$$-\langle uv\rangle = \nu_t\frac{\partial\langle U\rangle}{\partial y}$$

$$\nu_t = l_m^2\frac{\partial\langle U\rangle}{\partial y}$$

$$\frac{\partial\langle U\rangle}{\partial y} > \text{for BL}$$

Define

$$l_m^+ = l_m/\delta_\nu$$

And normalize Eq. (3) using y^+ and u^+ to obtain:

$$\frac{\tau}{\tau_w} = \frac{\partial u^+}{\partial y^+} + \left(l_m^+\frac{\partial u^+}{\partial y^+}\right)^2$$

$$\frac{\partial u^+}{\partial y^+} = \frac{2\tau/\tau_w}{1 + [1 + (4\tau/\tau_w)(l_m^+)^2]^{1/2}} \quad (4)$$

In the inner layer, $\tau/\tau_w \approx 1$ and the law of the wall can be expressed in terms of the mixing length as the integral of Eq. (4):

$$u^+ = f_w(y^+) = \int_0^{y^+}\frac{2dy^+}{1 + [1 + 4l_m^+(y^+)^2]^{1/2}} \rightarrow l_m^+ = f(y^+)$$

1) Log law region: $l_m^+ = ky^+ \rightarrow l_m = ky$
2) If $l_m^+ = ky^+$ in sublayer $\rightarrow -\langle uv\rangle^+ \approx {l_m^+}^2 = (ky^+)^2$, whereas $-\langle uv\rangle^+ \propto {y^+}^3$
3) $\therefore l_m^+$ requires damping:

$$l_m^+ = ky^+[1 - \exp(-y^+/A^+)]$$

Where $A^+ = 26$. Numerical integration shown in Fig 7.27 shows excellent agreement.

4) Large y^+, log law recovered $l_m^+ = ky^+$.
5) For $k = 0.41$ and $A^+ = 26$, $B = 5.3$.
6) Using Van Driest in sublayer gives:

$${l_m^+}^2 = \left(\frac{k}{A^+}\right)^2 {y^+}^4$$

i.e., better estimate than using $l_m^+ = ky^+$.

The velocity-defect law

In the defect layer ($y/\delta > 0.2$), the mean velocity deviates from log law, as per Fig. 7.27-7.28.

Mean velocity profile can be represented as the sum of two functions:

$$u^+ = \frac{\langle U\rangle}{u_\tau} = \underbrace{f_w(y^+)}_{\boxed{\text{law of the wall}}} + \underbrace{\frac{\Pi}{k} w\left(\frac{y}{\delta}\right)}_{\boxed{\text{law of the wake}}} \qquad (5)$$

Wake function: $w(y/\delta)$ Coles (1956), $w(0) = 0, w(1) = 2$.

$$w(y/\delta) = 2\sin^2\left(\frac{\pi}{2}\frac{y}{\delta}\right)$$

Based on EFD with $\Pi =$ wake strength parameter and flow dependent.

Fig. 7.28 $u^+ = f_w(y^+) + \frac{\Pi}{k} w\left(\frac{y}{\delta}\right)$ with $f_w(y^+) =$ log law.

The shape of the function $w(y/\delta)$ is like the velocity profile in a plane wake with symmetry plane at $y = 0$.

Alternatively, Eq. (5) can be written as a velocity-defect law:

$$\frac{U_0 - \langle U \rangle}{u_\tau} = \frac{1}{k}\{-\ln\left(\frac{y}{\delta}\right) + \Pi\left[2 - w\left(\frac{y}{\delta}\right)\right]\}$$

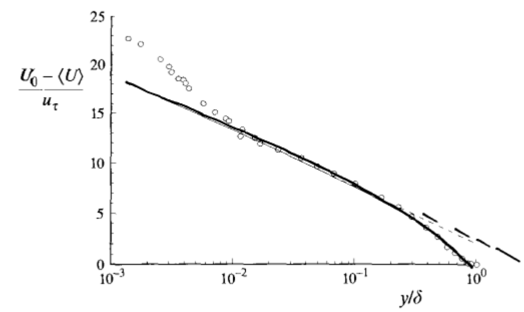

Fig. 7.29. The velocity-defect law. Symbols, experimental data of Klebanoff (1954); dashed line, log law; solid line, sum of log law and wake contribution $\Pi w(y/\delta)/\kappa$.

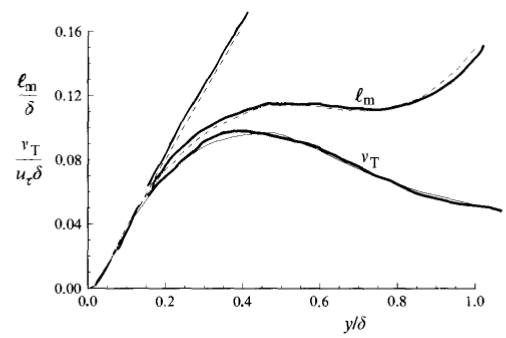

Fig. 7.30. Turbulent viscosity and mixing length deduced from direct numerical simulations of a turbulent boundary layer (Spalart 1988). Solid line, ν_T from DNS; dot–dashed line, ℓ_m from DNS; dashed line ℓ_m and ν_T according to van Driest's specification (Eq. (7.145)).

Evaluation of Eq. (5) at $y = \delta$ leads to a friction law:

$$\frac{U_0}{u_\tau} = \frac{1}{k}\ln\left(\frac{\delta u_\tau}{\nu}\right) + B + \frac{2\Pi}{k}$$

$$= \frac{1}{k}\ln\left(Re_\delta \frac{u_\tau}{U_0}\right) + B + \frac{2\Pi}{k}$$

$$Re_\delta = \frac{U_0 \delta}{\nu}$$

Solve for $u_\tau/U_0 \rightarrow c_f = 2(u_\tau/U_0)^2$

Power law fit:

$$c_f = 0.370(\log_{10} Re_x)^{-2.584}$$

In the defect layer $\tau < \tau_w$ (see Fig. 7.26) and $\langle U \rangle_y > u_\tau / ky$ as per log law. Therefore, $\nu_t = \tau / \langle U \rangle_y < u_\tau / ky$ as per log law.

Mixing length models: modify $l_m = ky$ in the defect layer, e.g., $l_m = \min(ky, 0.09\delta)$.

A Single Formula for the "Law of the Wall"

D. B. SPALDING[1]

Summary

It is shown that experimental velocity distributions may be well fitted, in the laminar sublayer, the transition region, and the turbulent core, by the formula:

$$y^+ = u^+ + 0.1108\{e^{0.4u^+} - 1 - 0.4u^+ - (0.4u^+)^2/2! - (0.4u^+)^3/3! - (0.4u^+)^4/4!\}$$

Omission of the $(0.4u^+)^4$ term gives an equally good fit. The corresponding expressions for the ratio of turbulent shear stress to total shear stress agree with the measurements of Laufer [8][2] quite closely.

(i) passes through the point: $y^+ = 0$, $u^+ = 0$;
(ii) is tangential at this point to: $u^+ = y^+$;
(iii) is asymptotic at large y^+ to:[4]

$$u^+ = 2.5 \ln y^+ + 5.5 \quad (2)$$

(iv) fits the experimental points at intermediate y^+ values.

Table 1 Formulas for the "law of the wall"[a]

Author	Range of validity	Formulas
Prandtl [11][b]	$0 \leqslant y^+ < 11.5$	$u^+ = y^+$
Taylor [18][b]	$11.5 \leqslant y^+$	$u^+ = 2.5 \ln y^+ + 5.5$
von Karman [7]	$0 \leqslant y^+ < 5$	$u^+ = y^+$
	$5 \leqslant y^+ < 30$	$u^+ = 5 \ln y^+ - 3.05$
	$30 \leqslant y^+$	$u^+ = 2.5 \ln y^+ + 5.5$
Reichardt [15]	$0 \leqslant y^+$	$u^+ = 2.5 \ln(1 + 0.4y^+) + 7.8\{1 - e^{-y^+/11} - (y^+/11)e^{-0.33y^+}\}$
Deissler [2]	$0 \leqslant y^+ < 26$	$u^+ = \int_0^{y^+} \frac{dy^+}{1 + n^2u^+y^+(1 - e^{-n^2u^+y^+})}$, $n = 0.124$
	$26 \leqslant y^+$	$u^+ = 2.78 \ln y^+ + 3.8$
van Driest [19]	$0 \leqslant y^+$	$u^+ = \int_0^{y^+} \frac{2dy^+}{1 + \{1 + 0.64y^{+2}[1 - \exp(-y^+/26)]^2\}^{1/2}}$
Rannie [13]	$0 \leqslant y^+ < 27.5$	$u^+ = 14.54 \tan h(0.0688y^+)$
	$27.5 \leqslant y^+$	$u^+ = 2.5 \ln y^+ + 5.5$

[a] See also Hofmann [5], Reichardt [14], Rotta [16], Miles [9], Elrod [3], and Frank-Kamenetsky [21].
[b] These authors did not, at the dates in question, state the formulas attributed to them in the table. However, they did introduce the idea of a sharp division between a laminar sublayer and a fully turbulent core; when compared with experimental data, this idea leads directly to the formulas given.

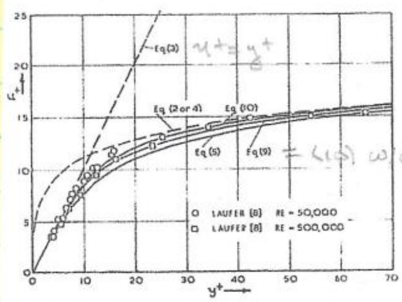

Fig. 1 Experimental data of Laufer [8] for velocity distribution near the wall in turbulent pipe flow, compared with various analytical expressions

Overlap region reconsidered.

$$\langle U \rangle_y = \frac{u_\tau}{y} \Phi_i \left(\frac{y}{\delta_\nu} \right)$$

i.e.,

$$y \frac{\partial u^+}{\partial y} \neq f(U_0, \delta, \nu) \sim f(Re)$$

$\delta_\nu = \nu / u_\tau$

$\frac{y}{\delta_\nu} = y^+$

Large $y^+ \rightarrow \Phi_i \neq f(\nu) \rightarrow \Phi_i(y^+) = \text{constant} = 1/k$

However,

$$\sqrt{\langle u^2 \rangle}, \sqrt{\langle v^2 \rangle} = f(Re)$$

In overlap region.

Consider weaker alternative assumptions. Velocity profile in inner layer:

$$u^+ = f_I(y^+)$$

Where f_I may depend on Re.

In the outer layer:

$$\frac{U_0 - \langle U \rangle}{u_0} = F_0(\eta)$$

Where $\eta = y/\delta$ and $u_0 \neq u_\tau$ and F_0 may depend on Re.

For overlap region $(\delta_\nu \ll y \ll \delta) \rightarrow f_I(\text{large } y^+) = F_0(\text{small } \eta)$

Two possibilities:

1) $u^+ = \frac{1}{k} \ln y^+ + B$
2) $u^+ = C(y^+)^\alpha$

With $\alpha, B, k, C > 0$, but may be $f(Re)$. If not $f(Re) \rightarrow$ universal laws.

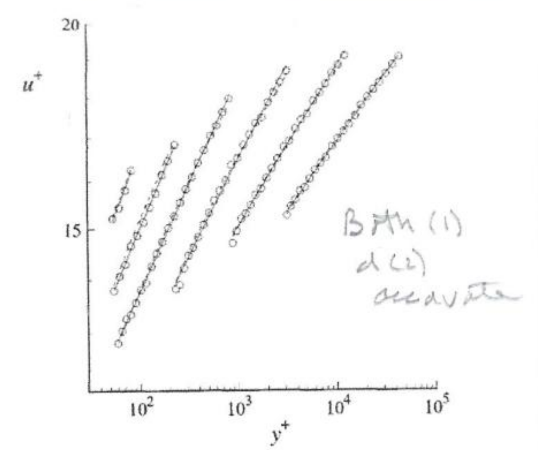

Fig. 7.31. A log–log plot of mean velocity profiles in turbulent pipe flow at six Reynolds number (from left to right: Re ≈ 32×10^3, 99×10^3, 409×10^3, 1.79×10^6, 7.71×10^6, and 29.9×10^6). The scale for u^+ pertains to the lowest Reynolds number: subsequent profiles are shifted down successively by a factor of 1.1. The range shown is the overlap region, $50\delta_\nu < y < 0.1 R$. Symbols, experimental data of Zagarola and Smits (1997); dashed lines, log law with $\kappa = 0.436$ and $B = 6.13$; solid lines, power law (Eq. (7.157)) with the power α determined by the best fit to the data.

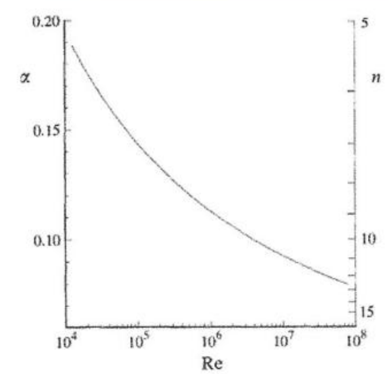

Fig. 7.32. The exponent $\alpha = 1/n$ (Eq. (7.158)) in the power-law relationship $u^+ = C(y^+)^\alpha = C(y^+)^{1/n}$ for pipe flow as a function of the Reynolds number.

$$\alpha = \frac{1.085}{\ln Re} + \frac{6.535}{(\ln Re)^2}$$

BL Reynolds Stresses, TKE budgets

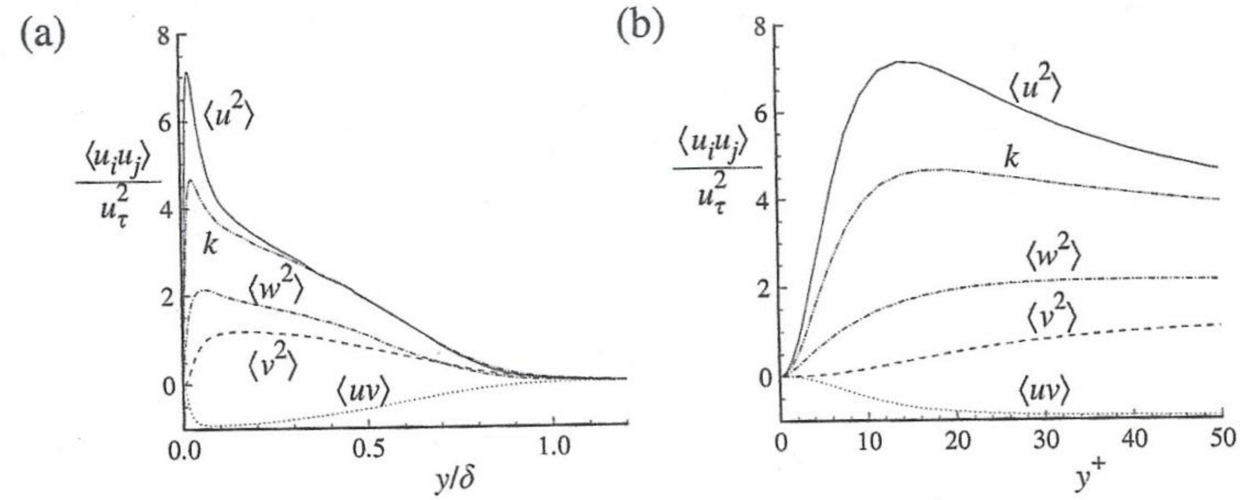

Fig. 7.33. Profiles of Reynolds stresses and kinetic energy normalized by the friction velocity in a turbulent boundary layer at $\mathrm{Re}_\theta = 1{,}410$: (a) across the boundary layer and (b) in the viscous near-wall region. From the DNS data of Spalart (1988).

Same trends as channel flow, but in this case merge with non-turbulent outer flow.

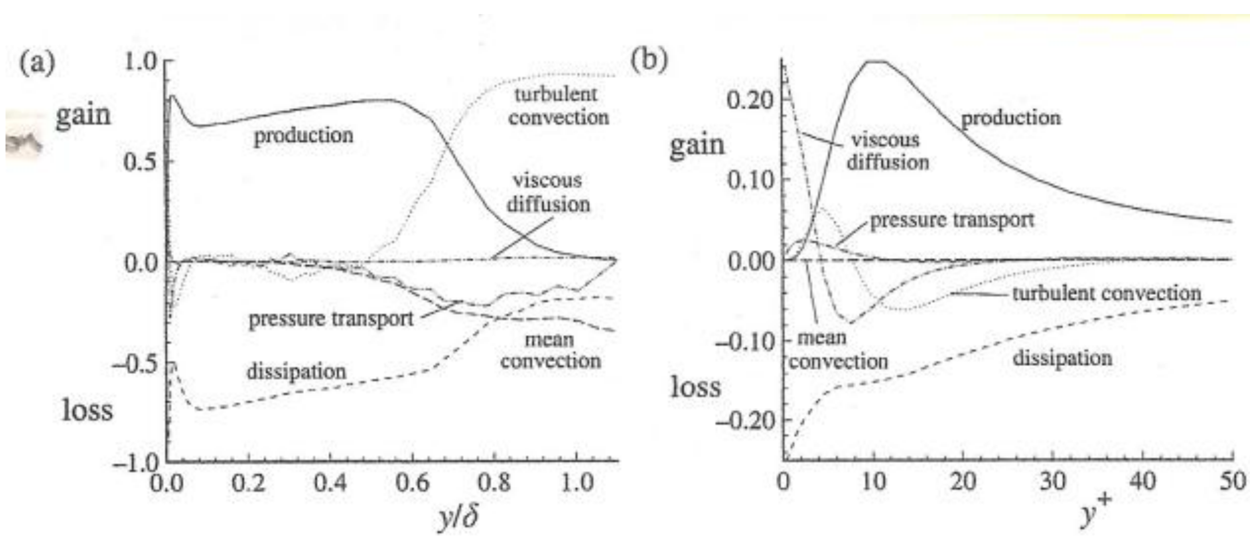

Fig. 7.34. The turbulent-kinetic-energy budget in a turbulent boundary layer at $\mathrm{Re}_\theta = 1{,}410$: terms in Eq. (7.177) (a) normalized as a function of y so that the sum of the squares of the terms is unity and (b) normalized by the viscous scales. From the DNS data of Spalart (1988).

TKE budget same channel flow, except the addition of the mean-flow-convection term:

$$\langle U\rangle\frac{\partial k}{\partial x}+\langle V\rangle\frac{\partial k}{\partial y}=P-\tilde{\varepsilon}+\nu\frac{\partial^2 k}{\partial y^2}-\frac{\partial}{\partial y}\langle\frac{1}{2}v\underline{u}\cdot\underline{u}\rangle-\frac{1}{\rho}\frac{\partial}{\partial y}\langle vp'\rangle \quad (6)$$

$y^+ \leq 50$ convection is negligible ∴ same trend channel flow.

For larger y/δ magnitude of terms in Eq. (6) decreases. The figure shows normalized values such that the sum of their squares is unity. From $y^+ \approx 40$ to $y/\delta \approx 0.4$, $P\sim\tilde{\varepsilon}$.

For $y/\delta > 0.4$, P small and balance is between dissipation and transport terms.

RS Budget

Transport equation for RS:

$$\frac{\bar{D}}{\bar{D}t}\langle u_i u_j\rangle=-\frac{\partial}{\partial x_k}\langle u_i u_j u_k\rangle+\nu\nabla^2\langle u_i u_j\rangle+P_{ij}+\Pi_{ij}-\varepsilon_{ij}$$

Where P_{ij} is the production tensor:

$$P_{ij}=-\langle u_i u_k\rangle\frac{\partial\langle U_j\rangle}{\partial x_k}-\langle u_j u_k\rangle\frac{\partial\langle U_i\rangle}{\partial x_k}$$

Π_{ij} is the velocity-pressure gradient tensor:

$$\Pi_{ij}=-\frac{1}{\rho}\langle u_i\frac{\partial p}{\partial x_j}+u_j\frac{\partial p}{\partial x_i}\rangle$$

ε_{ij} is the dissipation tensor:

$$\varepsilon_{ij}=2\nu\langle\frac{\partial u_i}{\partial x_k}\frac{\partial u_j}{\partial x_k}\rangle$$

It is possible to relate these symmetric second-order tensors to other quantities:

$$\frac{1}{2}P_{ii}=P$$

$$\frac{1}{2}\varepsilon_{ii}=\tilde{\varepsilon}$$

$$\frac{1}{2}\Pi_{ii}=-\frac{\partial}{\partial x_i}\langle u_i p/\rho\rangle$$

Normal-stress balances

Simple shear flow $\underline{U} = (U(y), 0,0)$, i.e., U_y is dominant mean velocity gradient.

$$P_{11} = 2P = -2\langle uv \rangle \frac{\partial \langle U \rangle}{\partial y}$$

$$P_{22} = P_{33} = 0$$

i.e., all kinetic energy production is in $\langle u \rangle^2$.

In TKE balance p appears as transport term and is relatively small, i.e.,

$$\frac{1}{2}\Pi_{ii} = -\nabla \cdot \langle \underline{u}p/\rho \rangle$$

Whereas Π_{ij} plays a central role: Π_{11} dominant sink in the $\langle u \rangle^2$ balance, Π_{22} and Π_{33} dominant source in $\langle v \rangle^2$ and $\langle w \rangle^2$.

Consequently, the primary effect of the fluctuating pressure is to redistribute energy from $\langle u \rangle^2$ to $\langle v \rangle^2$ and $\langle w \rangle^2$.

$$\Pi_{ij} = \mathcal{R}_{ij} - \frac{\partial}{\partial x_k} T_{kij}^{p}$$

Where $\mathcal{R}_{ij}$ is the pressure rate of strain tensor:

$$\mathcal{R}_{ij} \equiv \langle \frac{p}{\rho}\left(\frac{\partial u_i}{\partial x_j} + \frac{\partial u_j}{\partial x_i}\right) \rangle$$

And T_{kij}^{p} is the pressure transport:

$$T_{kij}^{p} \equiv \frac{1}{\rho}\langle u_i p \rangle \delta_{jk} + \frac{1}{\rho}\langle u_j p \rangle \delta_{ik}$$

$\mathcal{R}_{ii} = 0$ since $\nabla \cdot \underline{u} = 0$ $\therefore$ not in TKE equation.

In BL energy transfer at rate

$$-\mathcal{R}_{11} = \mathcal{R}_{22} + \mathcal{R}_{33}$$

From $\langle u \rangle^2$ to $\langle v \rangle^2$ and $\langle w \rangle^2$.

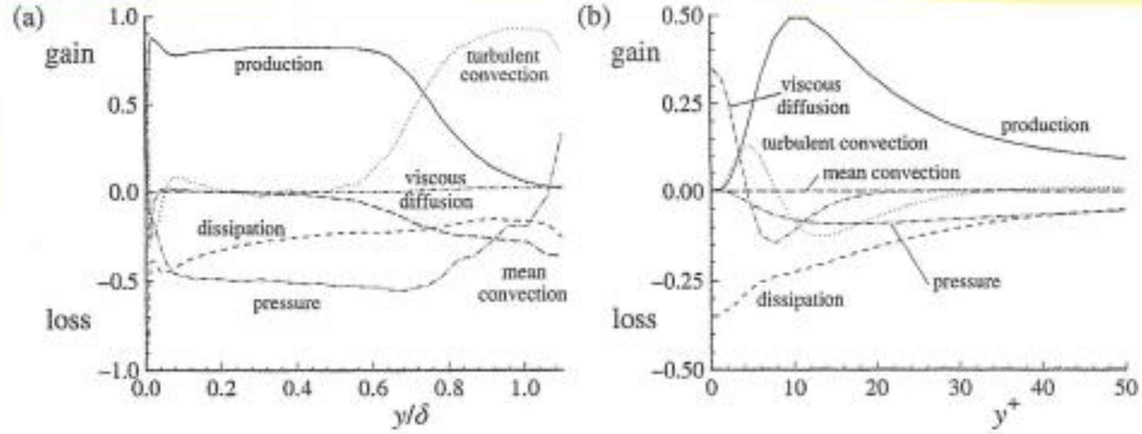

Fig. 7.35. The budget of $\langle u^2 \rangle$ in a turbulent boundary layer: conditions and normalization are the same as those in Fig. 7.34.

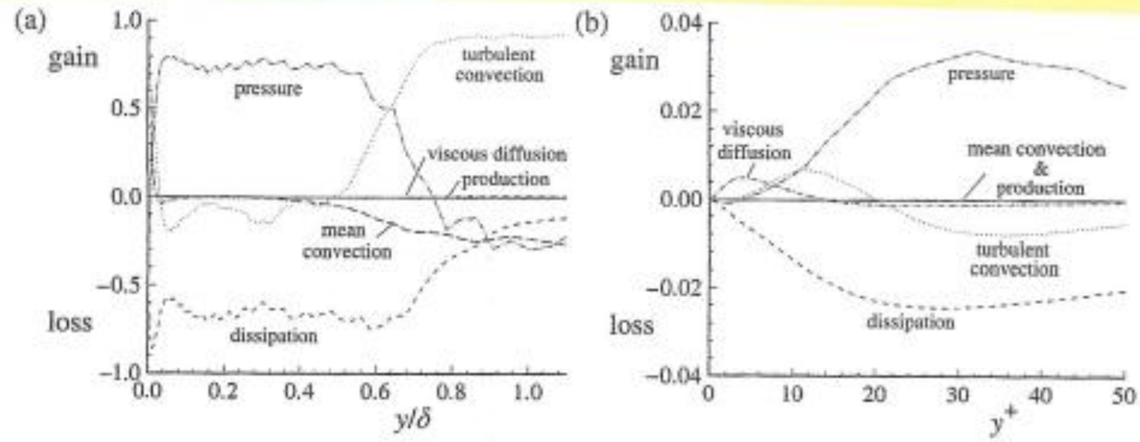

Fig. 7.36. The budget of $\langle v^2 \rangle$ in a turbulent boundary layer: conditions and normalization are the same as those in Fig. 7.34.

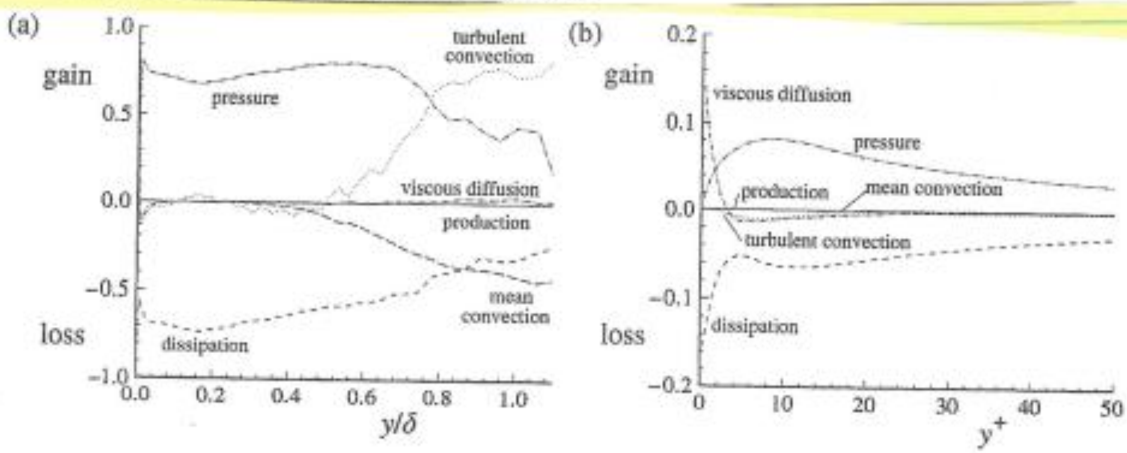

Fig. 7.37. The budget of $\langle w^2 \rangle$ in a turbulent boundary layer: conditions and normalization are the same as those in Fig. 7.34.

Shear Stress Balance

Since $\langle uv \rangle < 0$, a gain in $-\langle uv \rangle$ corresponds to an increase in magnitude of shear stress. From $y^+ \approx 40$ to $y/\delta \sim 0.5$, $-P_{12} = \langle v^2 \rangle \langle U_y \rangle = -\Pi_{12}$.

Differently from normal-stress balance, except near the wall, dissipation ε_{12} small.

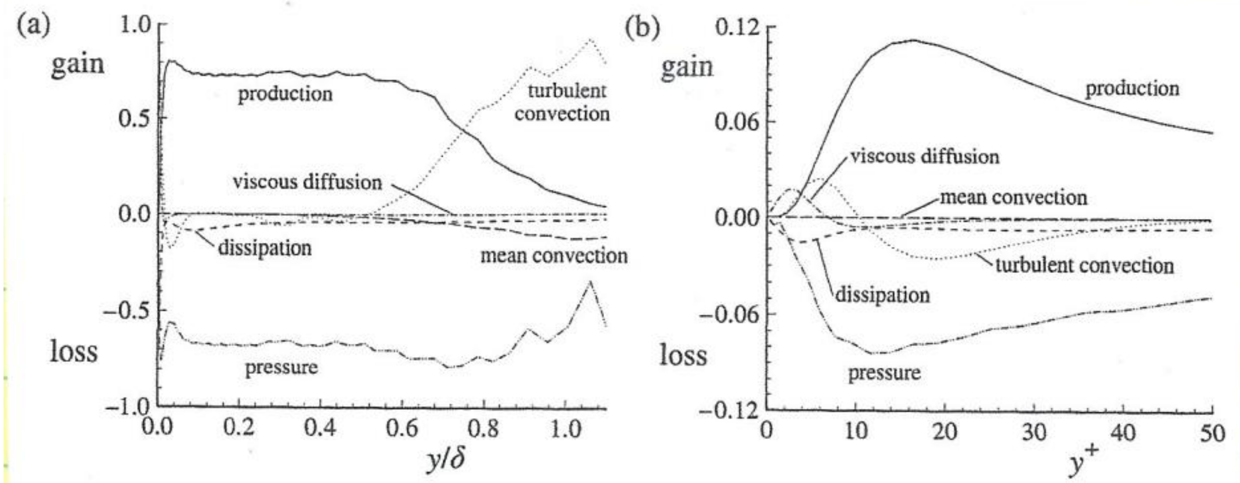

Fig. 7.38. The budget of $-\langle uv \rangle$ in a turbulent boundary layer: conditions and normalization are the same as those in Fig. 7.34.

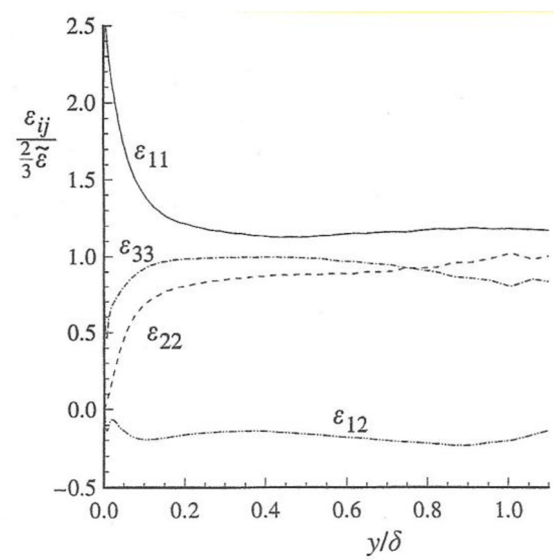

Fig. 7.39. Normalized dissipation components in a turbulent boundary layer at $Re_\theta =$ 1,410: from the DNS data of Spalart (1988), for which $\delta = 650\delta_\nu$.

From RS budget, it is clear that Π_{ij} is important along with P_{ij} and ε_{ij}.

Isotropic turbulence:

$$\varepsilon_{ij} = \frac{2}{3}\tilde{\varepsilon}\delta_{ij}$$

Close to wall ε_{ij} anisotropy is large, but for $y/\delta > 0.2$ $(y^{+} > 130)$ ε_{ij} almost isotropic, i.e.,

$$\frac{\varepsilon_{ij}}{\frac{2}{3}\tilde{\varepsilon}} \sim 1$$

For higher Re, ε_{ij} for $y/\delta > 0.1$ is isotropic.

$$\underbrace{\Delta U f(\eta)}_{\boxed{2}}$$